



Comment on “Exploring nature and predicting strength of hydrogen bonds: A correlation analysis between atoms-in-molecules descriptors, binding energies, and energy components of symmetry-adapted perturbation theory”

Sadisha Nanayakkara | Yunwen Tao | Elfi Kraka

Department of Chemistry, Southern Methodist University, Dallas, Texas, USA

CorrespondenceElfi Kraka, Department of Chemistry, Southern Methodist University, 3215 Daniel Avenue, Dallas, TX 75275-0314.
Email: ekraka@gmail.com**Abstract**

We evaluate the correlation between binding energy (BE) and electron density $\rho(r)$ at the bond critical point for 28 neutral hydrogen bonds, recently reported by Emamian and co-workers (*J. Comput. Chem.*, **2019**, *40*, 2868). As an efficient tool, we use local stretching force constant k_{HB}^a derived from the local vibrational mode theory of Konkoli and Cremer. We compare the physical nature of BE versus k_{HB}^a , and provide an important explanation for cases with significant deviation in the BE- k_{HB}^a relation as well as in the BE- $\rho(r)$ correlation. We also show that care has to be taken when different hydrogen bond strength measures are compared. The BE is a cumulative hydrogen bond strength measure while k_{HB}^a is a local measure of hydrogen bond strength covering different aspects of bonding. A simplified and unified description of hydrogen bonding is not always possible and needs an in-depth understanding of the systems involved.

KEYWORDS

binding energy, electron density, hydrogen bond, local hydrogen bond energy, local vibrational mode theory

In a recent article,¹ Emamian and co-workers judiciously selected a diverse collection of 42 hydrogen-bonded dimers including 28 neutral and 14 charged complexes, in order to study the nature of hydrogen bonds with quantum chemistry. The geometry of these 42 dimer complexes was optimized at B3LYP-D3(BJ)/ma-TZVPP level²⁻⁴ and the binding energies (BEs) characterizing the strength of H-bonding were calculated at CCSD(T)/jul-cc-pVTZ level^{5,6} employing half of basis set superposition error correction.^{7,8} The authors utilized symmetry-adapted perturbation theory (SAPT) at the SAPT2 + (3) δ MP2/aug-cc-pVTZ level⁹⁻¹¹ to decompose the BEs into energy components and proposed a novel classification of hydrogen bonding into four categories: *very weak*, *weak to medium*, *medium*, and *strong*. Emamian and co-workers observed fairly strong linear correlation between the CCSD(T) BEs and the electron density $\rho(r)$ at the (3,-1) hydrogen bond

critical point (BCP) for both the neutral ($R^2 = 0.9732$) and charged ($R^2 = 0.9644$) complexes. They advocated the use of this correlation between BE and $\rho(r)$ as a convenient way to predict in the molecular systems the BE of individual hydrogen bonds when these BEs are unattainable. We reassessed the correlation between BE and $\rho(r)$ for those hydrogen bonds in the 28 neutral complexes by utilizing the local vibrational mode theory^{12,13} and obtained interesting insights which provide a different perspective complementing the work of Emamian and co-workers.

As shown in Figure 1(A), the correlation between BE and $\rho(r)$ at the BCP of 28 neutral hydrogen bonds contains four cases with significant deviation identified with a deviation criterion of $1.5\cdot\sigma$ (σ is the standard deviation of the residuals after fitting). However, Emamian and co-workers did not provide any remarks on possible reasons.

In order to better understand and assess the above correlation, we employed the local vibrational mode theory originally developed

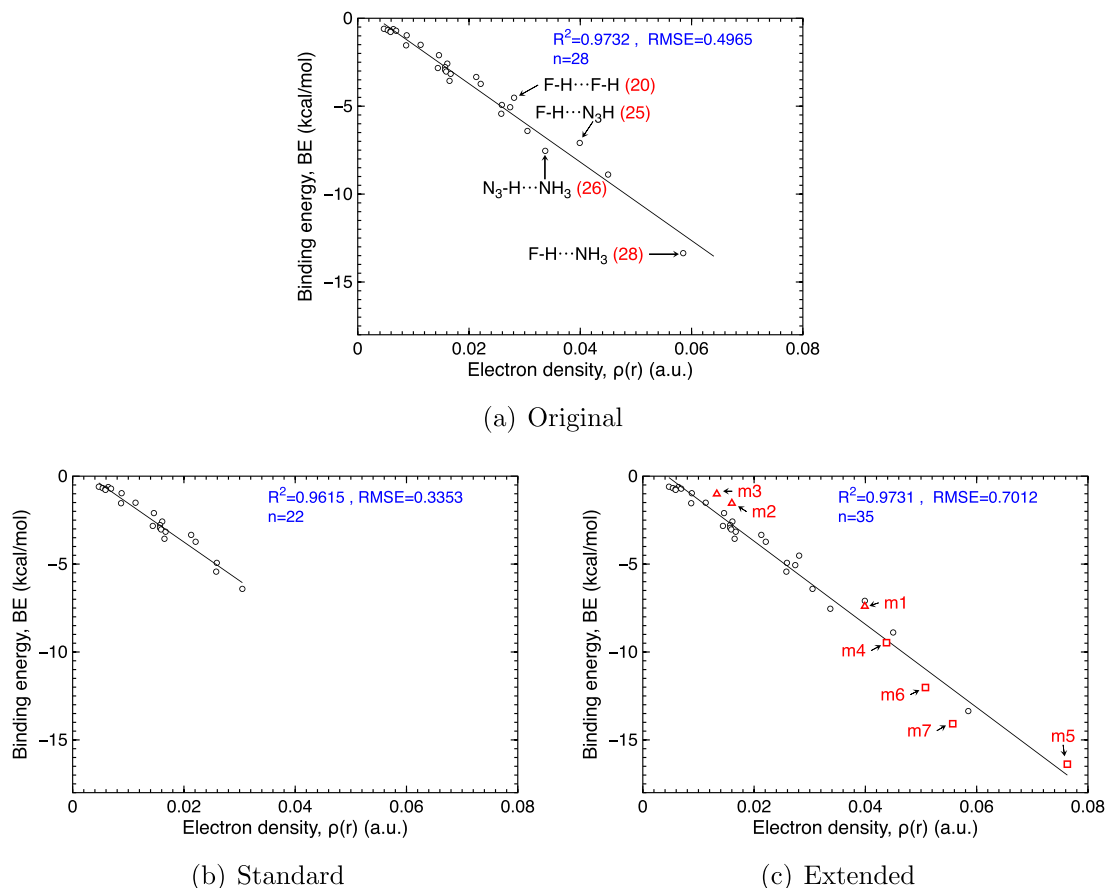


FIGURE 1 Correlation between BE and $\rho(r)$ at the BCP of the, (A) 28 neutral hydrogen bonds in the original dataset (reproduced from ref. [1]); (B) 22 neutral hydrogen bonds in the standard model or *Group 0*; (C) 35 neutral hydrogen bonds in the extended dataset. *Group 1+* and *Group 2+* dimers are represented by red triangles and squares, respectively. For a definition of *Group 0*, *Group 1+*, and *Group 2+*, see main text. *mi* ($i = 1-7$) denotes the new dimers. Coefficient of determination R^2 , standard deviation of the residuals RMSE, and the sample size n are indicated in blue for each linear regression line [Color figure can be viewed at wileyonlinelibrary.com]

TABLE 1 Local stretching force constant k_{HB}^a in $\text{mdyn}/\text{\AA}$ for the 28 neutral hydrogen bonds investigated by Emamian et al. in ref. [1]

Complex	k_{HB}^a	Complex	k_{HB}^a
1	0.018	15	0.095
2	0.025	16	0.098
3	0.026	17	0.099
4	0.028	18	0.099
5	0.028	19	0.127
6	0.027	20	0.177
7	0.042	21	0.167
8	0.054	22	0.176
9	0.049	23	0.164
10	0.066	24	0.195
11	0.082	25	0.251
12	0.094	26	0.194
13	0.088	27	0.315
14	0.092	28	0.372

Note: The ordering of these 28 complexes stays the same as the original work.

by Konkoli and Cremer to calculate the local stretching force constant k_{HB}^a of these 28 hydrogen bonds (collected in Table 1) based on the Hessian (second-order derivatives of energy) matrices of the equilibrium geometries optimized at the B3LYP-D3(BJ)/ma-TZVPP level.²⁻⁴ Konkoli and Cremer derived in 1998 the *local vibrational modes* associated with individual internal coordinates q_n (e.g., $\text{H}\cdots\text{A}$ hydrogen bond length in $\text{D}-\text{H}\cdots\text{A}$ hydrogen bonding) directly from the normal vibrational modes (within the harmonic approximation) by solving the mass-decoupled Euler-Lagrange equations.¹² The local vibrational mode associated with a bond stretching can be considered as the motion being obtained via an infinitesimal change in the bond length followed by the relaxation of all other atoms in the molecular system. Each local mode has its corresponding local mode frequency ω_n^a and local mode force constant k_n^a (subscript n represents the target internal coordinate parameter q_n). The local mode force constant is independent of atomic masses and characterizes pure electronic structure effects. The underlying physical nature of local mode force constant associated with a chemical bond is the curvature of the Born–Oppenheimer potential energy surface (PES) in the direction of the bond (i.e., diatomic) stretching. Therefore, the local stretching force constant has been extensively used to quantify the

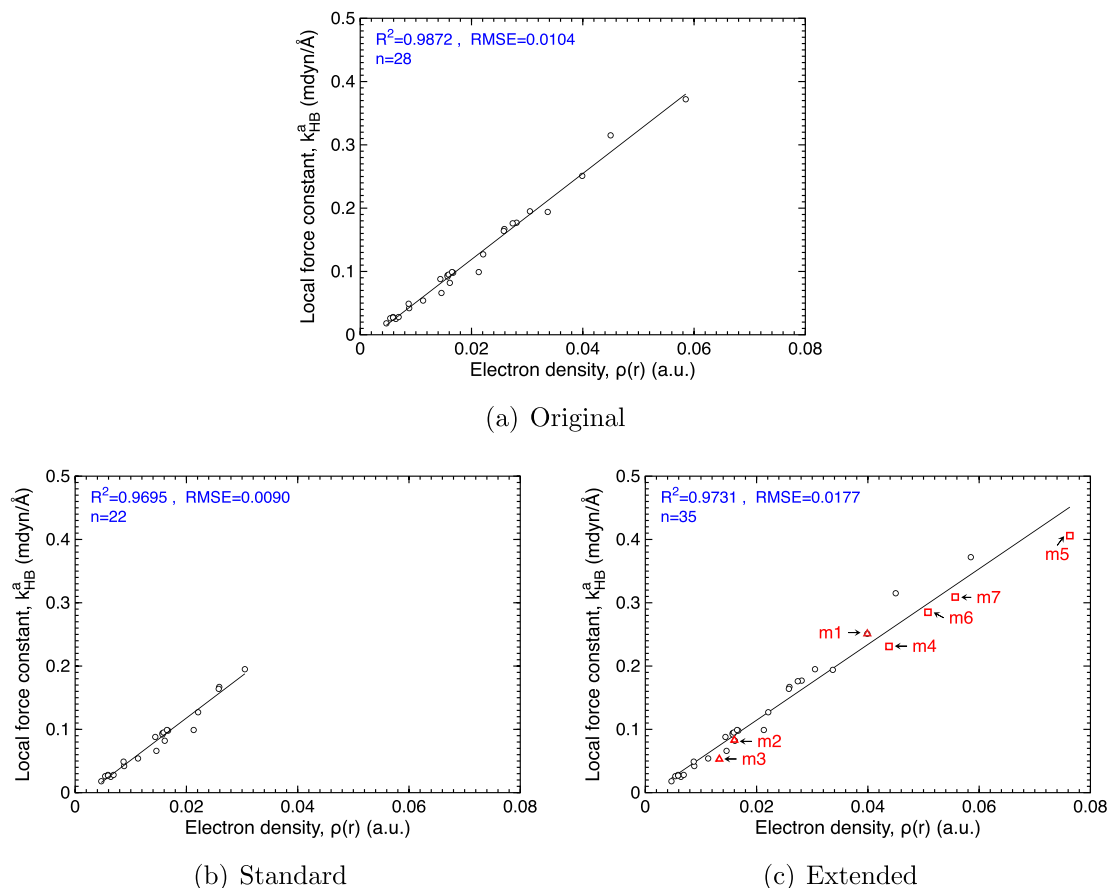


FIGURE 2 Correlation between local stretching force constant k_{HB}^a and $\rho(r)$ at the BCP of the, (A) 28 neutral hydrogen bonds in the original dataset; (B) 22 neutral hydrogen bonds in the standard model or *Group 0*; (C) 35 neutral hydrogen bonds in the extended dataset. *Group 1+* and *Group 2+* dimers are represented by red triangles and squares, respectively. For a definition of *Group 0*, *Group 1+*, and *Group 2+*, see main text. m_i ($i = 1-7$) denotes the new dimers. Coefficient of determination R^2 , standard deviation of the residuals RMSE, and the sample size n are indicated in blue for each linear regression line [Color figure can be viewed at wileyonlinelibrary.com]

intrinsic strength of both covalent bonds¹⁴⁻¹⁶ and noncovalent interactions including hydrogen,¹⁷⁻²⁰ halogen,²¹⁻²⁴ chalcogen,²⁵⁻²⁷ pnictogen,²⁸⁻³⁰ and tetrel bonding.³¹ Concerning the detailed mathematical derivation of local vibrational mode theory, interested readers are referred to a recent review article.¹³

We observed a rather strong correlation between the local stretching force constant k_{HB}^a and the electron density $\rho(r)$ at the BCP for the 28 neutral hydrogen bonds (see Figure 2(A)) and this correlation is marginally stronger than that between BE and $\rho(r)$ according to the coefficient of determination (R^2). For hydrogen bonding denoted as D-H...A (D: donor atom/group; A: acceptor atom/group), the (3, -1) BCP of hydrogen bond H...A is a point between two bonding atoms (H and A) where the first derivative of electron density vanishes (i.e., $\nabla\rho(r) = 0$) while the Hessian of dimension (3×3) for $\rho(r)$ has two negative eigenvalues and one positive eigenvalue.³² Furthermore, the local stretching force constant k_{HB}^a of the H...A hydrogen bond is the curvature of the PES in the direction of H...A stretching. Both $\rho(r)$ and k_{HB}^a are local second-order response properties associated with the H...A bond. This explains the strong correlation and also corroborates the fact that the local mode force constant characterizes the pure electronic structure effects.

The linear correlation between BE and local stretching force constant k_{HB}^a (see Figure 3(A)) is in the same range as the correlation between BE and $\rho(r)$. On one hand, Emamian and co-workers carefully picked small-sized molecules for their set of 28 neutral hydrogen bonded dimers with marginal secondary interactions, i.e. additional interactions between the two monomers besides the target hydrogen bonding, so that in this particular case the BE predominantly reflects the pure hydrogen bonding strength. On the other hand, the local stretching force constant k_{HB}^a with its physical nature as the curvature of PES in the direction of hydrogen bond stretching has been widely recognized as an intrinsic bond strength descriptor derived from vibrational spectroscopy.¹³ Therefore, it is of interest to check in more detail to what extent BE and k_{HB}^a as two different hydrogen bond strength descriptors are compatible with each other.

We got particularly interested in the five cases with significant deviation in the BE versus k_{HB}^a correlation identified with the deviation criterion of $1.5\cdot\sigma$ (see Figure 3(A)) because four of them overlap with the significantly deviated points in the BE versus $\rho(r)$ correlation. Before we delve into this, however, it is necessary to review the underlying physical nature of BEs when characterizing hydrogen bond strength, especially on what physical interactions are covered in

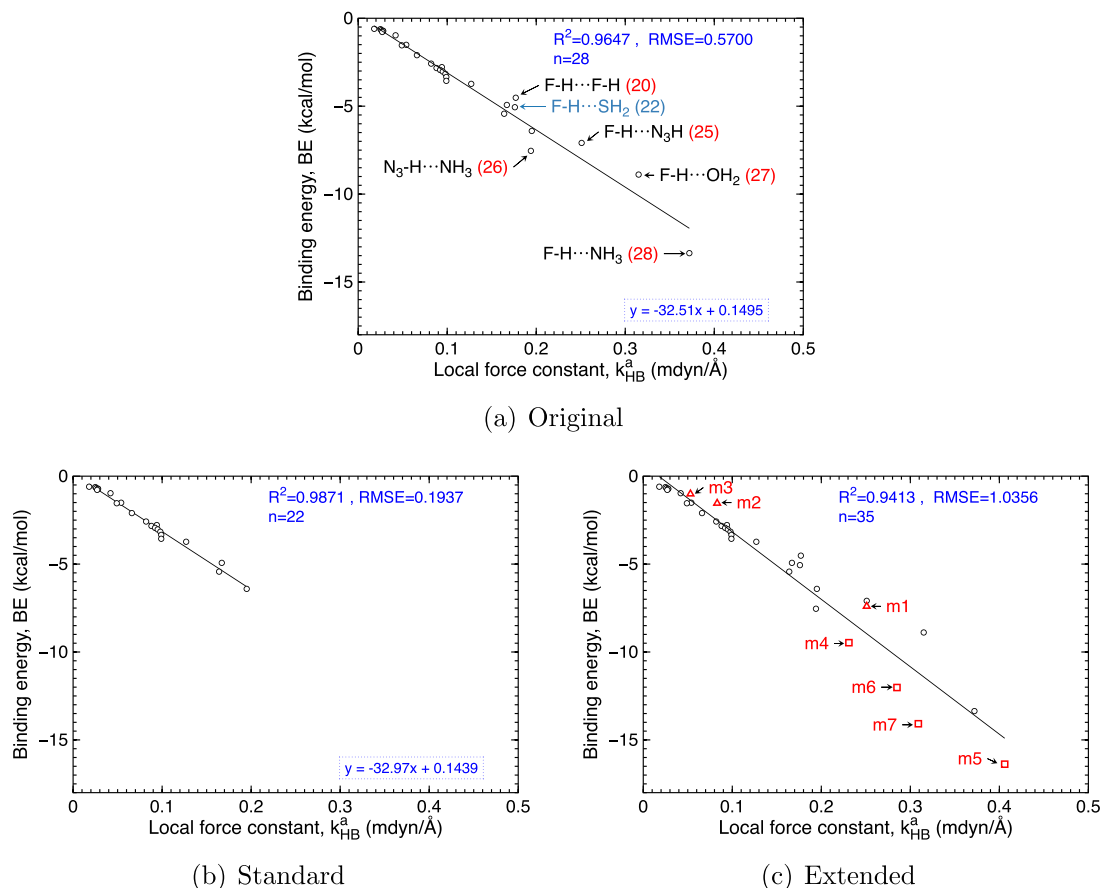


FIGURE 3 Correlation between BE and local stretching force constant k_{HB}^a of the, (A) 28 neutral hydrogen bonds in the original dataset; (B) 22 neutral hydrogen bonds in the standard model or *Group 0*; (C) 35 neutral hydrogen bonds in the extended dataset. *Group 1+* and *Group 2+* dimers are represented by red triangles and squares, respectively. For a definition of *Group 0*, *Group 1+*, and *Group 2+*, see main text. m_i ($i = 1-7$) denotes the new dimers. Coefficient of determination R^2 , standard deviation of the residuals RMSE, and the sample size n are indicated in blue for each linear regression line. Linear regression equations are shown for original and standard models [Color figure can be viewed at wileyonlinelibrary.com]



FIGURE 4 Schematic representation of a dimer system $\text{D-H}\cdots\text{A-R}$ stabilized by hydrogen bond $\text{H}\cdots\text{A}$. D-H is the donor monomer and D represent the atom/group covalently bonded to hydrogen. A is the acceptor atom/group and R is the rest part of the acceptor monomer. In this model, no secondary interaction between two monomers exists except the hydrogen bond. The local stretching force constant k_{HB}^a associated with hydrogen bond $\text{H}\cdots\text{A}$ covers the hydrogen bond interaction between these two monomers but it does not cover the additional (de)stabilization within monomers [Color figure can be viewed at wileyonlinelibrary.com]

comparison with local stretching force constants. Emamian and co-workers claimed¹ that the BE “is best to exhibit intrinsic binding strength of the monomers without considering the structural relaxation of the monomers.” In other words, the BE includes all energy contributions collectively upon complexation of the monomers. As we sketch in Figure 4, the local stretching force constant k_{HB}^a for $\text{H}\cdots\text{A}$

bond covers the pure hydrogen bond interaction connecting the two monomers, it does not cover additional interactions within the monomers caused by hydrogen bonding. Based on this analysis, we can explain the cases with significant deviation in the correlation between BE and k_{HB}^a shown in Figure 3(A).

The five points with significant deviation can be grouped into two parts including three above the regression line as *Group 1* and two below the regression line as *Group 2*. Additionally, *Group 0* refers to the standard model obtained after excluding *Group 1* and *Group 2*, which will be discussed in detail later. We find that *Group 1* complexes share the similarity that (1) the donor molecule is hydrogen fluoride and (2) the acceptor atom A has more than one lone pair available to delocalize into the $\sigma^*(\text{F-H})$ antibonding orbital. Since $\text{F-H}\cdots\text{SH}_2$ (complex 22) also has hydrogen fluoride as its hydrogen bond donor, it belongs to *Group 1*. The fluorine atom is extremely electronegative and therefore tends to attract F-H bonding electron density creating a partially positive charge on hydrogen atom. When hydrogen fluoride and the acceptor monomer is hydrogen bonded, the lone pair electrons from acceptor atom A delocalize into the $\sigma^*(\text{F-H})$ antibonding orbital. The delocalization is further strengthened by the pulling of the

TABLE 2 Binding energy (CCSD(T)/jul-cc-pVTZ level with half counterpoise correction, indicated as BE) in kcal/Mol, $\rho(r)$ (B3LYP-D3(BJ)/ma-TZVPP level) in a.u., local stretching force constant k_{HB}^a in mdyn/Å for the newly designed dimers

Group	Complex	Structure	BE	$\rho(r)$	k_{HB}^a
Group 1+	m1	FH...NCH	-7.40	0.0399	0.251
	m2	FH...OC	-1.54	0.0160	0.083
	m3	FH...FCCH	-1.01	0.0133	0.053
Group 2+	m4	N ₃ H...N(Me) ₃	-9.47	0.0438	0.231
	m5	FH...N(Me) ₃	-16.38	0.0763	0.406
	m6	HCOOH...NH ₃	-12.02	0.0508	0.285
	m7	HCO ₃ H ^a ...NH ₃	-14.08	0.0557	0.309

^aPeroxy acid.

electronegative fluorine atom. This provides the hydrogen atom in F—H with excess electron density leading to repulsive interaction with the electron density of the fluorine atom. Such a repulsion counting as a destabilizing factor toward the total BE is not reflected in the local stretching force constant k_{HB}^a explaining why these four data points are located above the regression line.

For *Group 2* complexes, the donor monomers are hydrogen azide (HN₃) and hydrogen fluoride (HF), both of which are weak acids while the acceptor monomer is ammonia (NH₃) as weak base. The association of ammonia and weak acid molecules reminds us of the formation of ammonium salt consisting of an ammonium cation (NH₄⁺) and an anion. Therefore, in the case of hydrogen bonding between ammonia (NH₃) and a weak acid (D—H), the partially ionic character of ammonium salt arising from the delocalization of ammonia lone pair into the σ^* (D—H) antibonding orbital (covalent character of H...N) leads to an electrostatic attraction between the anion (D⁻) and the ammonium cation (H⁺·NH₃).³³ Such an ionic attraction counts as a stabilizing factor toward the total BE but is not reflected by the local stretching force constant k_{HB}^a of H...N explaining why these two cases with significant deviation are found below the regression line.

Furthermore, to demonstrate that the observed deviations to the BE and k_{HB}^a model are not artifacts of the statistical method used here, but instead have a sound physical basis, we calculated BE, $\rho(r)$ (at the same levels of theory as in the ref. 1), and k_{HB}^a for a set of newly designed dimers (see Table 2). These were designed to have similar hydrogen bonding environment as in *Group 1* or *Group 2* dimers, which deviate from the simple hydrogen bond situation due to the presence of additional (de)stabilization. The new dimers contain as their acceptor or donor at least one of the monomers incorporated in the original 28 dimers. For a systematic comparison of how the presence of complexes that deviate from simple hydrogen bond situation can affect the quality of the BE and k_{HB}^a model, we did the following. First, we removed all the systems belonging to and as characterized by *Group 1* and *Group 2* dimer classes (i.e., *Group 1*: (20), (22), (25), (27), and *Group 2*: (26), (28), respectively) and only considered the rest of the 22 dimers (denoted as *Group 0*). These dimer systems have the simple situation in their hydrogen bonding nature and the corresponding linear regression line is considered as a standard/simple model between BE and k_{HB}^a , which has $R^2 = 0.9871$ with

RMSE = 0.1937 (see Figure 3(B)). Then, with the inclusion of the seven new dimers (denoted by *Group 1+* and *Group 2+*) we did linear regression for the extended data set with 35 dimers, and the corresponding linear regression line between BE and k_{HB}^a has $R^2 = 0.9413$ with RMSE = 1.0356 (see Figure 3(C)). In comparison to the standard model between BE and k_{HB}^a , we could still see a fairly high correlation for the extended data set, but the deviation (given by RMSE) is much more pronounced now. This is a clear indication that in the presence of complexes that diverge from the simple hydrogen bond situation, the quality of the model is affected and as a caveat we like to point out that careful consideration should be taken when presenting a unified picture of hydrogen bonding under such circumstances. Also, this analysis further confirmed, the identification of the deviations defined as *Group 1* and *Group 2*, is not merely based on the points produced by the statistical method we used here, but rather guided by our chemical intuition. A similar kind of evaluation was also carried out for BE and $\rho(r)$, and k_{HB}^a and $\rho(r)$ relationships as shown in Figures 1(B),(C) and 2(B),(C), respectively.

The conclusions of our work can be summarized as follows.

- Those cases with significant deviation in the $\rho(r)$ versus BE correlation are difficult to explain in reminiscence of the Hohenberg–Kohn theorem which relates energy to electron density, but so far the actual functional between the two is still not known. The local stretching force constant k_{HB}^a of hydrogen bond H...A characterizing the hydrogen bond strength between the donor and acceptor monomers is an effective tool for assessing cases with significant deviation in the BE- k_{HB}^a and BE- $\rho(r)$ correlations.
- For 28 neutral hydrogen-bonded dimer complexes investigated by Emamian and co-workers, both BE and k_{HB}^a are reasonable descriptors for quantifying the hydrogen bond strength and they provide in general consistent ordering of bond strength for these 28 complexes. We show that both BE and k_{HB}^a provide similar measures of hydrogen bond strength based on the judicious selection of donor/acceptor monomers forming 28 simple dimer complexes made by Emamian and co-workers. However, the local stretching force constant k_{HB}^a avoids the twist of borrowing additional local descriptors to indirectly quantify the hydrogen bond strength (like the use of $\rho(r)$ to predict BE). Therefore, the use of k_{HB}^a is straightforward

when measuring the hydrogen bond strength and generally applicable also to complex systems like water clusters or proteins.

- Our work provides a different point of view into the nature of hydrogen bonding by emphasizing the interactions within the donor/acceptor monomer which are not reflected by local electronic structure descriptors of $H \cdots A$ such as $\rho(r)$ and k_{HB}^a but contribute marginally to the total BE of the 28 neutral hydrogen-bonded complexes. Therefore, care has to be taken when different hydrogen bond strength measures are compared. The BE is a cumulative hydrogen bond strength measure while k_{HB}^a is a local measure of hydrogen bond strength.
- As a caveat we want to highlight, any attempt to present a simplified and unified description of hydrogen bonding as done in the work of Emamian and co-workers via their BE and $\rho(r)$ model, can be clouded by the fact that many systems tend to diverge from the simple hydrogen bond situation due to other factors that come into play. Thus, careful consideration should be taken under such situations.

ACKNOWLEDGMENTS

This work was financially supported by National Science Foundation Grants CHE 1464906. The authors thank SMU for providing super-computing resources. Yunwen Tao thanks Yue Qiu for helpful discussions.

DATA AVAILABILITY STATEMENT

The data that support the findings of this study are available from the corresponding author upon reasonable request.

ORCID

Elfi Kraka  <https://orcid.org/0000-0002-9658-5626>

REFERENCES

- [1] S. Emamian, T. Lu, H. Kruse, H. Emamian, *J. Comput. Chem.* **2019**, *40*, 2868.
- [2] L. Goerigk, S. Grimme, *J. Chem. Theory Comput.* **2010**, *7*, 291.
- [3] F. Weigend, R. Ahlrichs, *Phys. Chem. Chem. Phys.* **2005**, *7*, 3297.
- [4] J. Zheng, X. Xu, D. G. Truhlar, *Theor. Chem. Acc.* **2010**, *128*, 295.
- [5] R. J. Bartlett, *J. Phys. Chem.* **1989**, *93*, 1697.
- [6] E. Papajak, J. Zheng, X. Xu, H. R. Leverentz, D. G. Truhlar, *J. Chem. Theory Comput.* **2011**, *7*, 3027.
- [7] S. Boys, F. Bernardi, *Mol. Phys.* **1970**, *19*, 553.

- [8] L. A. Burns, M. S. Marshall, C. D. Sherrill, *J. Chem. Theory Comput.* **2013**, *10*, 49.
- [9] T. M. Parker, L. A. Burns, R. M. Parrish, A. G. Ryno, C. D. Sherrill, *J. Chem. Phys.* **2014**, *140*, 094106.
- [10] T. H. Dunning, *J. Chem. Phys.* **1989**, *90*, 1007.
- [11] D. E. Woon, T. H. Dunning, *J. Chem. Phys.* **1993**, *98*, 1358.
- [12] Z. Konkoli, D. Cremer, *Int. J. Quantum Chem.* **1998**, *67*, 1.
- [13] E. Kraka, W. Zou, Y. Tao, *WIREs: Comput. Mol. Sci.* **2020**, *10*, e1480.
- [14] E. Kraka, J. A. Larsson, and D. Cremer. in *Computational Spectroscopy* (Ed: J. Grunenberg), Wiley, New York **2010**, p. 105.
- [15] R. Kalescky, E. Kraka, D. Cremer, *J. Phys. Chem. A* **2013**, *117*, 8981.
- [16] W. Zou, D. Cremer, *Chem. – Eur. J.* **2016**, *22*, 4087.
- [17] R. Kalescky, W. Zou, E. Kraka, D. Cremer, *Chem. Phys. Lett.* **2012**, *554*, 243.
- [18] M. Freindorf, E. Kraka, D. Cremer, *Int. J. Quantum Chem.* **2012**, *112*, 3174.
- [19] Y. Tao, W. Zou, J. Jia, W. Li, D. Cremer, *J. Chem. Theory Comput.* **2017**, *13*, 55.
- [20] Y. Tao, W. Zou, E. Kraka, *Chem. Phys. Lett.* **2017**, *685*, 251.
- [21] V. Oliveira, E. Kraka, D. Cremer, *Phys. Chem. Chem. Phys.* **2016**, *18*, 33031.
- [22] V. Oliveira, E. Kraka, D. Cremer, *Inorg. Chem.* **2016**, *56*, 488.
- [23] V. P. Oliveira, E. Kraka, F. B. C. Machado, *Inorg. Chem.* **2019**, *58*, 14777.
- [24] Y. Tao, Y. Qiu, W. Zou, S. Nanayakkara, S. Yannacone, E. Kraka, *Molecules* **2020**, *25*, 1589.
- [25] D. Setiawan, E. Kraka, D. Cremer, *J. Phys. Chem. A* **2015**, *119*, 9541.
- [26] V. Oliveira, D. Cremer, E. Kraka, *J. Phys. Chem. A* **2017**, *121*, 6845.
- [27] V. Oliveira, E. Kraka, *J. Phys. Chem. A* **2017**, *121*, 9544.
- [28] D. Setiawan, E. Kraka, D. Cremer, *Chem. Phys. Lett.* **2014**, *614*, 136.
- [29] D. Setiawan, E. Kraka, D. Cremer, *J. Phys. Chem. A* **2014**, *119*, 1642.
- [30] D. Setiawan, D. Cremer, *Chem. Phys. Lett.* **2016**, *662*, 182.
- [31] D. Sethio, V. Oliveira, E. Kraka, *Molecules* **2018**, *23*, 2763.
- [32] R. F. W. Bader, *Atoms in Molecules: A Quantum Theory (International Series of Monographs on Chemistry)*, Clarendon Press, Oxford, UK **1994** ISBN 0198558651.
- [33] P. Gilli, L. Pretto, V. Bertolasi, G. Gilli, *Acc. Chem. Res.* **2009**, *42*, 33.

How to cite this article: Nanayakkara S, Tao Y, Kraka E.

Comment on “Exploring nature and predicting strength of hydrogen bonds: A correlation analysis between atoms-in-molecules descriptors, binding energies, and energy components of symmetry-adapted perturbation theory”.

J Comput Chem. 2020;1–6. <https://doi.org/10.1002/jcc.26475>